Bioactive Materials 4 (2019) 236–244

Contents lists available at ScienceDirect

Bioactive Materials

journal homepage: http://www.keaipublishing.com/biomat

In vitro and in vivo biocompatibility of Mg–Zn–Ca alloy operative clip

Pengfei Ding[a], Yuanchao Liu[b], Xianghui He[b], Debao Liu[c,*], Minfang Chen[d]

[a] School of Materials Science and Engineering, Tianjin University of Technology, Tianjin, 300384, China
[b] Tianjin Medical University General Hospital, Department of General Surgery, Tianjin, 300384, 300070, China
[c] National Demonstration Center for Experimental Function Materials Education, Tianjin University of Technology, Tianjin, 300384, China
[d] Tianjin Key Laboratory for Photoelectric Materials and Devices, Tianjin, 300384, China

ARTICLE INFO

Keywords:
Mg-Zn-Ca alloy
Biodegradable hemostatic clip
In vitro and in vivo biocompatibility
Carotid artery

ABSTRACT

At present, titanium (Ti) and its alloys are most commonly use in hemostasis clip clinical applications. However, the Ti Clip cannot be absorbed in human body and produce artifacts on computed tomography (CT), and induce clinically relevant hypersensitivity in patients. In order to overcome the drawbacks of the non-degradable Ti clips, an Mg–Zn–Ca alloy operative clip was fabricated by combining hot extrusion and blanking processing. In vitro and in vivo biocompatibility of Mg–Zn–Ca alloy operative clip were evaluated by L-929 Cells and SD rat model respectively. It was found that Mg–Zn–Ca alloy exhibited non-cytotoxic to L929 cells. In vivo implantation showed that the newly designed Mg–Zn–Ca clip can successfully ligated carotid artery and no blood leakage occurred post-surgery. During the period of the clip degradation, a small amount of H_2 gas formation and no tissue inflammation around the clips were observed. The degradation rate of the clip near the heart ligated the arteries faster than that of clip far away the heart due do the effect of arterial blood. Histological analysis and various blood biochemical parameters in rat serum samples collected at different times after clip implantation showed no tissue inflammation around the clips.

1. Introduction

Minimally invasive surgery has received increasing attention due to the minimization of tissue damage and more rapid postoperative recovery [1–3]. During the operation, blood vessels are usually occluded by using hemoststic clips instead of medical sutures because of the small surgical incision [4]. At present, titanium (Ti) and its alloys are most commonly used in clinical applications because they possess excellent ductility and biocompatibility to ensure occluding blood vessels completely and safely in biological systems [5–7]. However, in actual operation, there are many shortcomings influencing the reliability of hemostatic clips. Firstly, the corrosion rate of Ti alloys is so slow that Ti clips may remain in the body permanently and it is very difficult to remove the clips from dense tissues after a patient has fully recovered. In addition, removing the clips may result in secondary injuries and pain to patient [8,9]. Moreover, the X-ray scanning diagnosis will be interfered by Ti alloy clips due to its higher X-ray absorption coefficient compared to human tissue [8–10]. They can also cause allergic reactions and induce clinically relevant hypersensitivity in patients [11].

In order to overcome the drawbacks of the non-degradable Ti clips, it is expected that future hemostatic clips will only exist in the body temporarily. With the completion of the hemostatic function and the progress of tissue repair, it is possible for the clips to gradually degrade and for the body to absorb the degradation products. For example, Lapro-Clips can be fully hydrolyzed in 180 days without affecting the patient's medical examination post-operatively [12]. However, due to the low mechanical strength and elasticity modulus of polymer clips, clinically-used degradable polymer clips rely on a special structural design to ensure the sufficient clamping force resulting in a relatively complex clip structure, which increases the difficulty of surgical manipulation and greatly reduces the application range of biodegradable polymer clip.

Currently, magnesium and its alloys have received increasing attention as metallic implant materials due to their excellent biocompatibility and biodegradability. To date, magnesium alloys have been extensively studied in biodegradable bone fracture fixation, cardiovascular stents and other applications [13]. At present, the major drawback of the magnesium alloys as implant materials is that they dissolve too fast and promote fast degradation of mechanical properties before the completion of bone-healing process [14]. Although several methods such as alloying, high purification and surface modification treatments have been used to improve the corrosion resistance, this

Peer review under responsibility of KeAi Communications Co., Ltd.
* Corresponding author.
E-mail address: debaoliu@126.com (D. Liu).

https://doi.org/10.1016/j.bioactmat.2019.07.002
Received 20 March 2019; Received in revised form 17 July 2019; Accepted 30 July 2019
Available online 05 August 2019

problem still has not been solved effectively. From the perspective of service performance requirements for application in hemostasis clips, it is necessary to maintain the mechanical strength of the alloy for only two weeks, and therefore the rapid corrosion is not a major issue for the use of magnesium alloys. It was also shown that magnesium alloys did not exhibit artifacts in the CT testing [15]. Thus, magnesium and magnesium alloys are very desirable candidate materials for use in degradable hemostatic clips. However, pure Mg showed poor ductility due to the movement of some slip systems were limited by the high anisotropy of crystal structure [16]. When clip was occluded, a dramatic plastic deformation occurs at the top corner of the clip, which may lead to crack nucleation and propagation. Micro-cracks will be prone to corrode after implantation in the body, possibly leading to crevice corrosion and giving rise to clip fracture during the application period. On the other hand, alloying Mg with biocompatible elements and controlling the microstructure may contribute to the excellent fracture toughness of the Mg-based alloys. In recent years, Mg–Zn–Ca series alloys have attracted extensive attention. This is because both Zn and Ca are essential elements in the human body and are biocompatible within certain limits [17]. Moreover, these alloying elements are effective grain refiners for magnesium and therefore are expected to improve the ductility [18]. Recently, Mg-0.55Zn-0.16Ca clip was fabricated by double extrusion combined machining and manually bent processing route. This Mg-0.55Zn-0.16Ca clip successfully occluded renal vein in a rat model. There was no inflammation of the surrounding tissues [19]. However, the preparation process of the Mg-0.55Zn-0.16Ca clip is is relative complex, and the precision of the finished clip and the production efficiency need to be improved. Our previous work shows that Mg–3Zn-0.2Ca alloy exhibits the good combination of mechanical performance and corrosion resistance [17]. In this study, a new designed Mg–3Zn-0.2Ca alloy clip was fabricated by a novel route of combined hot extrusion and blanking process technology. After fabrication, these clips ligated carotid artery in a rat model. Microstructure evolution, mechanical properties, corrosion behavior and occlusion properties of the Mg–Zn–Ca alloy hemostatic clip were investigated in vitro and in vivo [20]. The biocompatibility evaluations of biodegradable Mg–Zn–Ca alloy hemostatic clips at different times after clip implantation were also investigated.

2. Material and methods

2.1. Structural dimension design for Mg–Zn–Ca alloy clip

The Structural dimension of the newly designed hemostatic clip is shown in Fig. 1. Compared with the reported Mg-0.55Zn-0.16Ca clip [19], the advantages of newly designed hemostatic clip are mainly manifested in two aspects. Firstly, the circular opening at the top of the clip is smaller, which makes it easier to fit the blood vessel wall during the operation and easier to clamp the blood vessel. Moreover, the two ends of the hemostatic clip are designed to be increasing thickness from the tail end to the top, which is mainly because the deformation stress of the clip is concentrated at the top, so as to avoid the top fracture during hemostatic clamping.

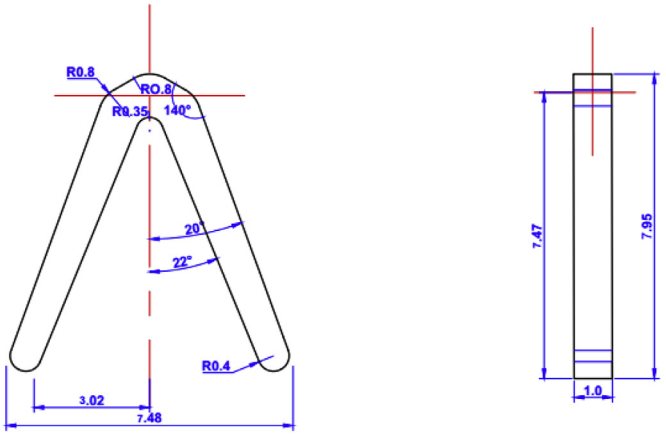

Fig. 1. Structural dimensions of Mg–3Zn-0.2Ca alloy clip.

Table 1
Nominal and analyzed compositions of Mg–3Zn-0.2Ca alloy.

	Mg-3 (wt.%) Zn-0.2 (wt.%) Ca		
	Mg	Zn	Ca
Nominal composition/wt.%	96.8	3.0	0.2
Analysis composition/wt.%	96.77	3.02	0.21

2.2. Sample preparation

High-purity magnesium ingot (99.99 wt%), Zn particles (99.99 wt %) and Mg–Ca master alloy (30 wt% Ca) were used as raw materials for the preparation of the Mg-3wt%Zn-0.2 wt%Ca alloy. The alloy was melted in a vacuum electromagnetic induction furnace (ZG-10, Shanghai, China) with mechanical agitation under the protection of argon gas at 720 °C. The molten metal was poured into a copper mold for casting. The composition of the Mg–3Zn-0.2Ca is also shown in Table 1.

The cast ingot was annealed at 380 °C for 24 h to homogenize the alloy, and then extruded as cylindrical bar (8 mm diameter) and rectangular sheet (45 mm wide × 1.1 mm thick) using a YQ 32–315 extruding machine at 320 °C. For cellular viability/cytotoxicity experiments, the bar-shaped alloys were cut into discs with heights of 3 mm or 0.5 mm. Blanking process was applied to cut the magnesium alloy sheets into clips with the shape and size shown in Fig. 1. The longer direction of the clip was parallel to the extrusion direction. Then, the clips were annealed at 300 °C for 2 h. Finally, all clips were polished to 1 mm thick and then ultrasonic cleaned in anhydrous ethanol and distilled water before drying and sterilization with gamma rays.

2.3. In vitro cell test

2.3.1. Indirect contact cytotoxicity test

L-929 Cells (Dingguo, China) cultured in RPMI-1640 medium (Gibco, US) supplemented with 10% fetal bovine serum (FBS) (Hyclone, US) were passaged 3 days and incubated at 37 °C and 5% CO_2 in a humidified incubator. Preparation of extracts were prepared according to ISO 10993-5 standard [21]. Disinfected cylinder alloy samples (Ø8 mm × 3 mm) were rinsed with phosphate buffer solution (PBS) (Sorabio, China) three times and then immersed in 1 mL RPMI-1640 medium supplemented with 10% FBS (the surface-to-volume ratio was 200 mm^2/mL) for 7 days in a 5% CO_2 humidified incubator at 37 °C. Fresh cell culture medium was added to dilute extracts of Mg–3Zn-0.2Ca alloy to 6.25%, 12.5%, 25% and 50%. RPMI-1640 medium containing 10% FBS was used as a negative control. Cells (5000 cells/well) were seeded in 96-well plates (Corning, USA) with cultivation media (RPMI-1640 medium + 10% FBS) and the plates were incubated at 37 °C and 5% CO_2 in a humidified atmosphere for 24 h to ensure cell attachment. The medium in each well was then exchanged with 100 μL extraction medium at different concentration (6.25%, 12.5%, 25%, 50% and 100%) and 100 μL pristine medium (negative control group) and the passaged cells continued to incubate for 1, 3 and 5 days in the same conditions. During this period, cell growth was observed by optical microscopy (Nikon ECLIPSE Ti inverted microscope, Japan) at the end time point of each group.

Cell viability was evaluated using MTT colorimetric assay (3-(4, 5-Dimethylthiazol-2-yl)-2, 5-diphenyltetrazolium bromide) (Sigma, US).

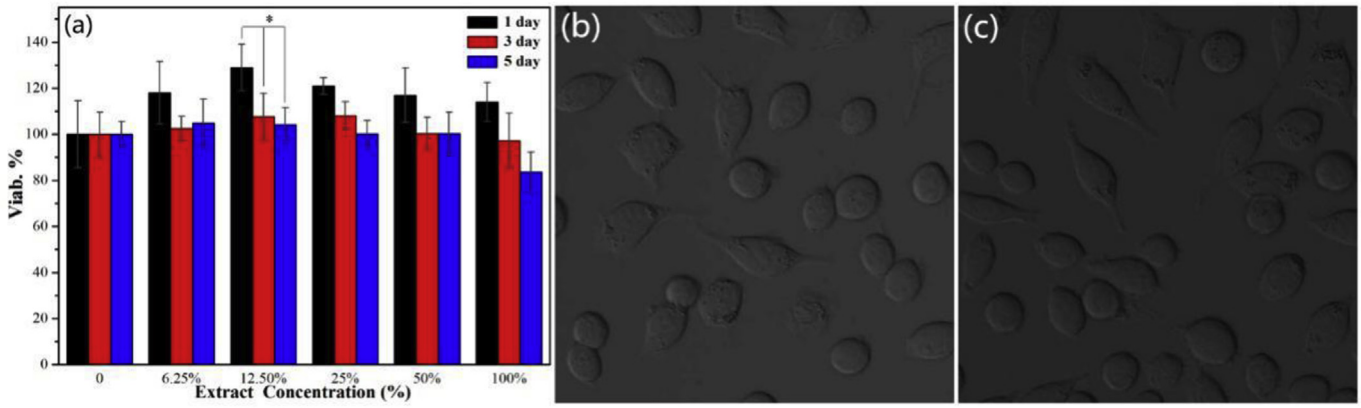

Fig. 2. (a) The viability of L929 cells exposed to different concentrations of immersion extracts (0, 6.25%, 12.5%, 25%, 50%, 100% Mg–3Zn-0.2Ca alloy) and times (1, 3, 5 days), *: $p < 0.05$. The typical morphologies of L929 cells cultured in RPMI-1640 medium +10% FBS (b) and 12.5% Mg–3Zn-0.2Ca alloy extract (c) for 5 days.

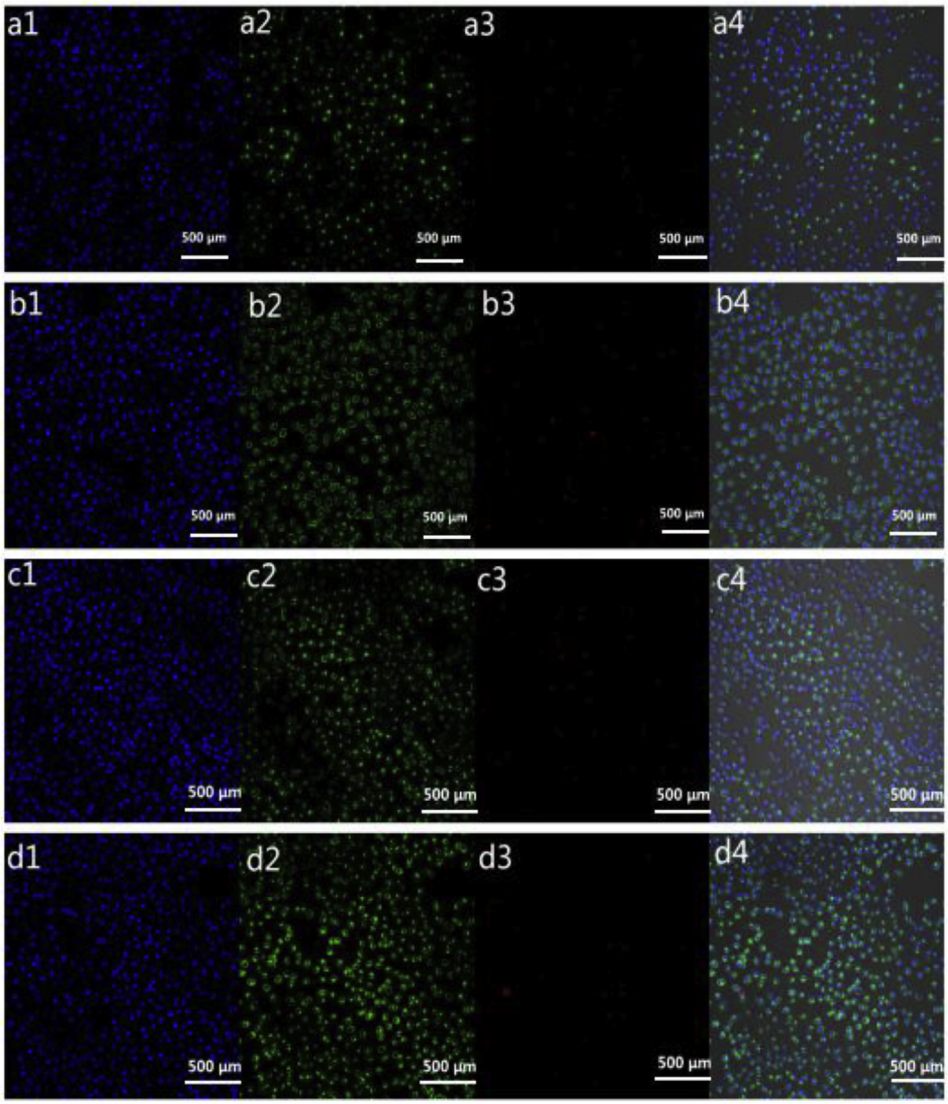

Fig. 3. Morphologies of direct growth of L929 cells: cells were stained after seeding on Mg–3Zn-0.2Ca substrates for one day (a1-a4) or five days (b1-b4); cells were stained after seeding on plastic tissue culture sample for one day (c1-c4) or five days (d1-d4). Living cells fluoresced green and dead cells fluoresced red.

20 μL MTT solution (dissolved in PBS, 5 mg/mL) was added to each test well and then incubated for 3h (37 °C, 5% CO2, 95% relative humidity). Finally, 150 μL dimethylsulfoxide (DMSO) (Sorabio, China) was added to each well and optical density (OD) measurements were conducted using an Epoch spectrophotometer (Bio-Tek, US) at 570 nm after another 10 min incubation at room temperature. The change in cell

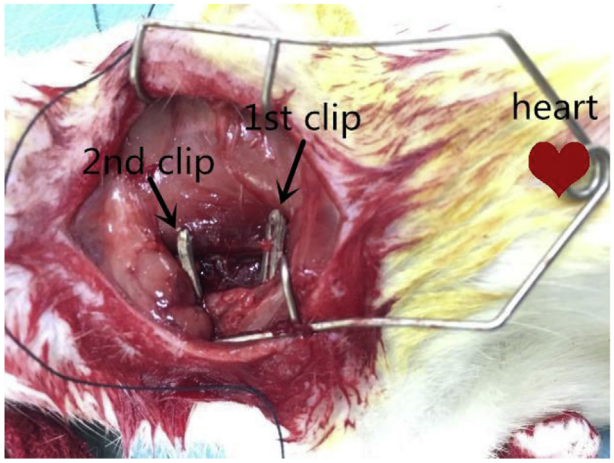

Fig. 4. Clip occluded carotid blood vessels of rats showing no blood leakage post-surgery.

viability compared to the negative control was calculated according to the following equation: Viab.% = ODtest/ODnegative × 100%.

According to ISO 10993-5 standards, the value of Viab.% was converted into a grade between 0 and V to assess the cytotoxic potential of each sample: 100% or more is grade 0, 75%–99% is I, 50%–74% is II, 25%–49% is III, 1%–24% is IV and 0% is V. Extracts causing a Viab.% reduction greater than grade I were considered cytotoxic to cells, as described in ISO 10993–5 [21].

2.3.2. Direct cell adhesion experiments

500 μL L929 cells were seeded on bare Mg–Zn–Ca substrates (Ø8 mm × 0.5 mm) and plastic tissue culture substrates (Ø8 mm × 0.5 mm) at a seeding density of 5 × 105 cell/mL in six-well plates. The plates were maintained at 37 °C and 5% CO_2 in a humidified atmosphere for 48 h. To assess living and dead cells on the surface of the sample, all test discs were washed with abundant PBS and marked with Hoechst 33342, Propidium Iodide (PI, Sigma–Aldrich, Missouri, USA) and Wheat Germ Agglutinin (WGA) stains. The specific methods of cell staining are as follows. Firstly, blue fluorescent Hoechst 33342 was added to each well at a concentration of 5 μg/mL and incubated for 15 min, which penetrated the cell membrane of living and dead cells. Next, dead cells were labelled with 20 μg/mL PI for at least 10 min at room temperature. PI stain cannot penetrate intact cell membranes, so only necrotic cells with a loss of cell membrane integrity produced red fluorescence. Finally, 5 μg/mL WGA was dropped in each well, which produced green fluorescence in healthy cells. The treated cells were observed by optical microscopy (Nikon ECLIPSE Ti inverted microscope).

2.4. In vivo safety estimation

2.4.1. Surgical procedure

All animal studies were approved by the Institutional Animal Care and Ethics Committee of Tianjin Medical University General Hospital and carried out in this hospital (Permission number: SYXK:2016–0012). The sterilized clips were used in 15 healthy 8 weeks old SD rats (Sprague-Dawley) with average weight of 300 ± 5g to investigate the ability to clinically occlude blood vessels. All rats were randomly separated into five groups according to implantation time of 0.5, 1, 1.5, 2 and 3 months. General anesthetic was performed using an intramuscular injection of 10% chloral hydrate (0.3 mL/100 g) for SD rats. The rat's neck was disinfected with iodine. Afterwards, the rat was placed in a supine position and the neck was covered with a sterile drape to provide sterile conditions during operation. A 6 cm incision was made into the skin and neck tissue to expose the left common carotid. The blood vessel was ligated twice by the clips using the specific hemostatic clip applier and then cut in-middle. After the procedure, the carotid artery was observed for 10 min to confirm complete hemostasis and no blood leakage. The jugular incision was washed by 0.9% NaCl solution and closed by medical suture.

2.4.2. X-ray scanning

Ventro-dorsal digital radiographs of rats' neck were taken to record the closure and degradation of implanted hemostatic clips. The X-ray machine (Digital Diagnost, Philips, Amsterdam, Netherlands) was operated under the following conditions: 52 kV, 3.2 mAs and 10.9 ms. X-rays were performed at 0.5, 1, 1.5, 2 and 3 months after surgery to assess the blood vessel healing and the degradation of clips. The rat was anesthetized with 10% chloral hydrate (0.3 mL/100 g) intramuscularly before each X-ray scanning.

2.4.3. Blood biochemistry

Blood samples were gathered prior to operation and at 0.5, 1, 1.5, 2 and 3 months after surgery. Blood biochemical tests were performed to evaluate white blood cell count and concentrations of alanine aminotransferase (ALT), aspartate transaminase (AST), creatinine (CRE), urea and Mg ion.

2.4.4. Autopsy and histologic analysis

After implantation for 0.5, 1, 1.5, 2 and 3 months, the SD rats were sacrificed by a painless procedure and immediately autopsied to determine the healing effect of the severed blood vessel and adhesion condition around the clips. The clips and surrounding tissues were explanted. After various implantation periods, the surface morphology and chemical composition of explanted clips were characterized by scanning electron microscopy (SEM, Tescan Vega 3) with an energy dispersion spectrometer (EDS, Oxford Instruments Inca 350). Degradation products were washed off by CrO3 solution (200 g/L) and the weight loss (mg) of the clips were measured and recorded. The tissue around the hemostatic clip was separated and fixed in a 10% formalin solution, embedded in solid paraffin, and then cut into 3 μm thick slices. After Hematoxylin–Eosin (HE) and Sirius Red (SR) staining, routine pathological examinations were performed to assess the degree of inflammation.

2.5. Statistical analysis

All data is expressed as a mean value ± standard deviation (showed with error bars in figures). A statistically significant difference between groups was considered to $p < 0.05$.

3. Results and discussion

3.1. Cytotoxicity test

Cells culture is a very useful in vitro method to detect the interaction between cells and biological materials. To investigate the effect of the corrosion products of biodegradable Mg–3Zn-0.2Ca alloy on cell growth, the viability of L929 cells exposed to different concentrations of Mg–3Zn-0.2Ca alloy immersion extracts and exposure durations were examined (Fig. 2a). Cultured L929 cells showed greater viability with Mg–3Zn-0.2Ca alloy extracts compared with the negative control group and no statistically significant difference ($P < 0.05$) of cell viability was detected between immersed extract dilutions. Viab.% values increased firstly and then decreased with increasing extract concentrations. The highest cell viability was measured in 12.5% extract cultures. Cell viability above 100% was observed when L929 cells were cultured in lower concentrations of extracts (6.25%,12.5%,25%) for 1 day, which may be due to the promotion effect of magnesium hydroxide in the corrosion products. When both the concentration of the cultivation fluid increased (100%) and the culture time increased (> 3 days), the cell viability was reduced due to the high concentration of extracts

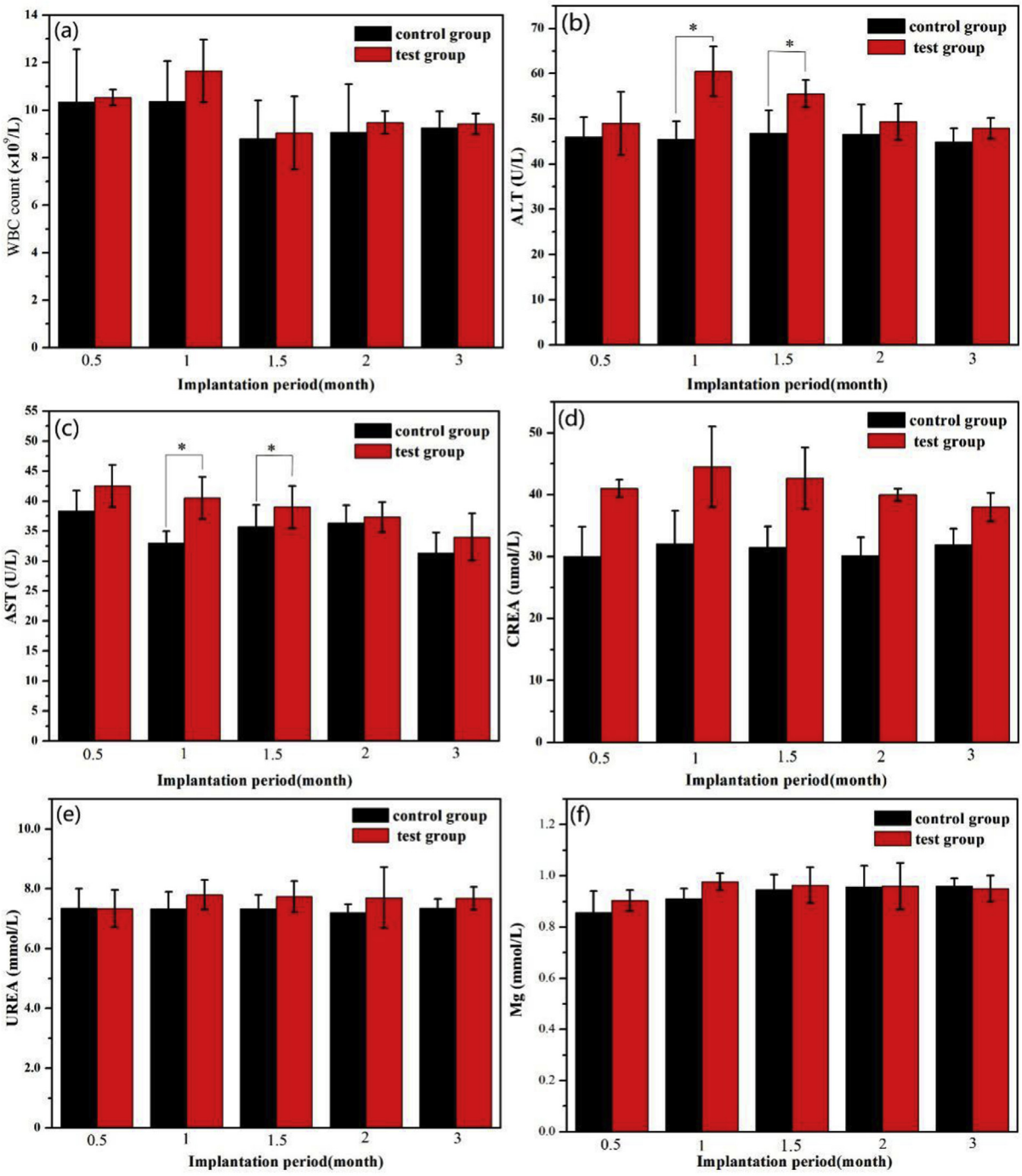

Fig. 5. Blood biochemical values in mouse serum: (a) white blood cell count, (b) alanine aminotransferase (ALT), (c) aspartate transaminase (AST), (d) creatinine (CREA), (e) urea and (f) Mg ion, *: $p < 0.05$.

leading to osmotic shock of the cells temporarily. After culturing for 5 days in 100% extracts, the viability value of the cells reached a minimum value of 85%. The cytotoxicity of these extracts was still at grade 0 to I (ISO 10993–5), which suggests the L929 cells were well tolerated in various concentrations of Mg–Zn–Ca extracts. Fig. 2b and c shows the typical morphologies of L929 cells cultured for 5 days in RPMI-1640 medium +10% FBS and 12.5% extracts, receptively. All cells exhibited normal circular and spindle morphology, which indicates the cells were healthy and could be sub-cultured normally.

To study the direct growth of L929 cells that attached on bare Mg–3Zn-0.2Ca alloys, 500 μL cells suspensions (5×10^5 cell/mL) were seeded on Mg–3Zn-0.2Ca substrates and plastic tissue culture sample. The cells were stained by three steps according to the method described in section 2.2.2 after one and five days of incubation and observed with optical microscopy (Fig. 3). L929 cells cultured on both substrates were abundant and evenly dispersed (Fig. 3. (a1,a2,b1,b2,c1,c2,d1,d2)), few apoptotic cells were observed on each sample (Fig. 3. (a3,b3,c3,d3)). The morphologies of the L929 cells stained by the three staining reagents were shown in Fig. 3.(a4,b4,c4,d4). After 1 day in culture, the elongated and expanded morphology of adherent cells on the Mg–Zn–Ca alloys confirmed cellular compatibility with the alloy. No obvious differences in cell morphology were observed between these two groups, so the corrosion of Mg alloys did not inhibit cell adhesion. The cell density was similar among the Mg–3Zn-0.2Ca alloys despite

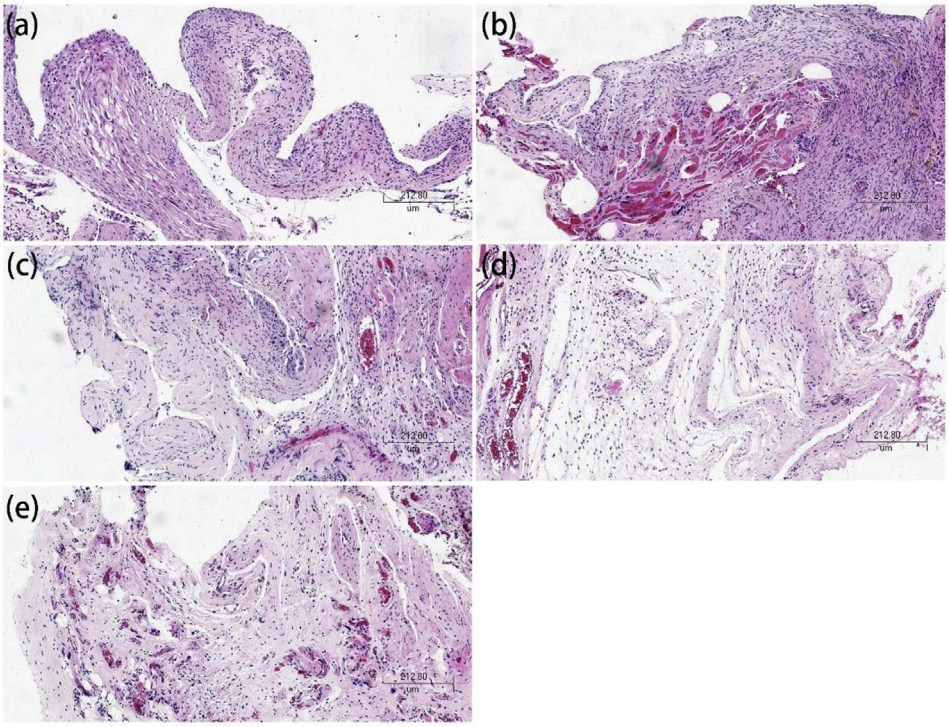

Fig. 6. Histological analysis of tissue around clips following implantation for (a) 0.5, (b) 1, (c) 1.5, (d) 2 and (e) 3 months.

different cell culture time, indicating the cells were not significantly affected by prolonged direct exposure times to the corrosion environment. Thus, the surface of Mg–3Zn-0.2Ca alloy allowed cells to attach and maintain for a longer period of time. However, more dead cells were found on the surface of the experiment alloys when compared to the negative control group. This result may be related to the higher corrosion rate and the accumulation of corrosion products from Mg alloys. This result was consistent with the 5-day MTT assessments at 25% and 50% extract concentrations where cell viability was lower than the negative control. The direct cell adhesion experiments indicated that Mg–3Zn-0.2Ca alloy possesses similar cytocompatibility to tissue culture plastic sample. Therefore, these results showed the cells could be attached, spread and proliferated on the Mg–3Zn-0.2Ca alloy effectively and healthily.

3.2. In vivo safety evaluation

3.2.1. Evaluation for occlusion of blood vessel

Surgeries of the left common carotid artery closure were performed as described in section 2.3.1. One set of clips was used on the blood vessel near the heart as shown in Fig. 4. There was no blood leakage after surgery and the total time from incision to closing the incision was no more than 30 min. All SD rats survived the operation and recovered with no obvious complications during the predefined observation period, indicating the Mg–3Zn-0.2Ca clip possessed sufficient occlusion property. Our previous studies showed that the yield tensile strength (0.2%YS), ultimate tensile strength and elongation of extruded Mg–3Zn-0.2Ca alloys were 205 MPa, 336 MPa and 17.85%, respectively, which ensure the complete closure of the clips during surgery [17,18].

3.2.2. Evaluation for blood biochemistry parameters

Fig. 5 shows the Mg ion concentration and five blood biochemical parameters in rat serum samples collected at different times after clip implantation. The serum levels of ALT, AST ($p < 0.05$) and CREA slightly increased after operation, but there were almost no differences in these indicators when compared with the control group after longer implantation times. In the clinic, AST and ALT are used as criteria for the detection of liver function in organisms. In addition, CREA is an indicator for renal function. The ratios of AST and ALT ($p < 0.05$) in post-surgical blood samples were all less than 1, indicating that the implantation of clips had limited effects on the liver function of the rats. CREA levels were in the range of normal values (44–80 μmol/L) after 3-months implantation, therefore the effect on renal function was also limited. Since human beings are much larger than rats, we can infer that the implantation of these clips will have little impact on human health.

3.2.3. Histological analysis

Hematoxylin-eosin stained tissues around the clips after implantation for 0.5, 1, 1.5, 2 and 3 months are shown in Fig. 6. After implantation for 0.5 months, no obvious signs of adverse inflammatory reactions were found in the tissues surrounding the clips (Fig. 6a). The staining slice after implantation for one month (Fig. 6b) shows the number of macrophages and lymphocytes increased and mild fibrosis can be seen in the tissue, which suggests some inflammation occurred during this period. After one month, less fibrotic and inflammation was observed in the connective tissue microscopically suggesting the rat's immune system had a lower rejection rate of the clips after the longer implantation period.

3.2.4. Degradation behavior of Mg–Zn–Ca alloy clips

Fig. 7 shows X-ray images of implanted clips after 0.5, 1, 1.5, 2 and 3 months, and yellow circle marks the location of the clip in each rat. It was found that these is no obvious metallic artifacts, indicating the implanted Mg clips had no effect on the CT imaging. At 0.5 months after operation, the clip can be clearly identified and some black area surrounding clips is observed, which indicates H_2 gas generation in the initial period of degradation.

Magnesium and its alloys degrade in aqueous environments, generating magnesium (Mg^{2+}) and hydroxide (OH^-) ions, as well as hydrogen (H^2) gas. Hydrogen has certain solubility and diffusion coefficient in blood and muscle, so it can be absorbed by surrounding tissues by dissolution and diffusion. Comparatively, no dark area was found around the clips after implantation for more than 0.5 months,

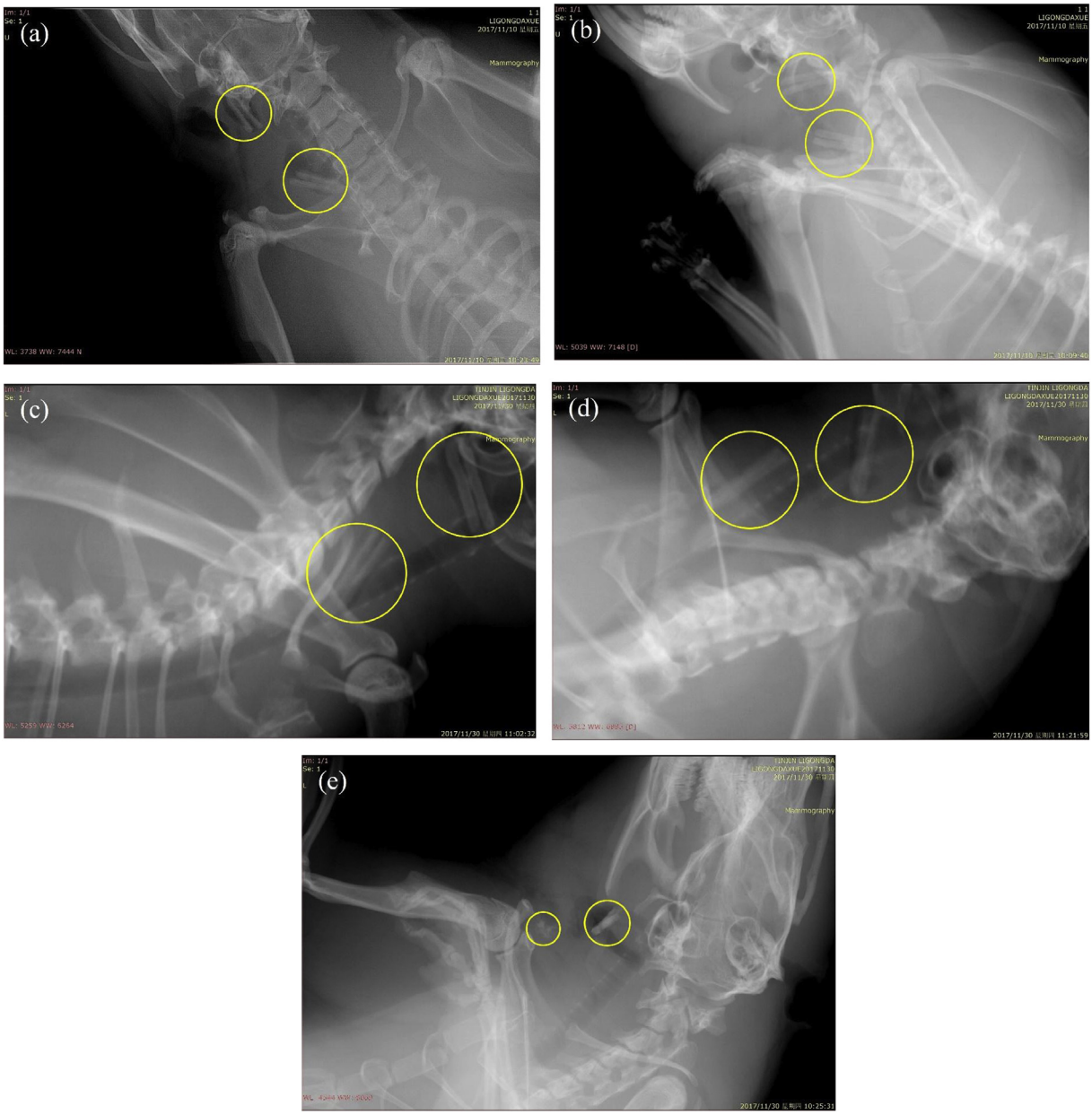

Fig. 7. X-ray images of clips implant after (a) 0.5, (b) 1, (c) 1.5, (d) 2 and (e) 3 months. Yellow circles mark the location of the clip in each rat.

indicating the degradation rate of the clip decreased as the implant time increases. One possible explanation for these results is that a fiber package may form between the surrounding tissue and the clip, which reduces the contact between the clip and the tissue fluid, thereby slowing down the degradation of the clip and reducing H_2 production. Throughout the two-month implantation period, the outline of the clips maintain basically, which could provide enough strength support to fully close blood vessels. After 3 months, some pieces of broken clip were observed on the side near the heart and the other clip was clearly identified. We also found the degradation rate of the clip near the heart faster than that of clip far away from the heart. That is because the clip connected to the heart and carotid, so the clip will continue to be affected by arterial blood, i.e. pulsating stress. It was reported that corrosions of Mg and its alloys are sensitive to stress and stress can accelerate Mg corrosion and cause stress corrosion cracking (SCC) [22–24]. In this study, pulsating stress accelerate Mg clip corrosion degradation, which is need consideration for the design and clinical application of Mg-based clip. On the contrary, the clip far away from the heart will no longer pump blood and will not be influenced by blood pressure. Thus, the degradation rate is relative slower.

Fig. 8a and d presents SEM images of two clips after implantation for two months. No significant changes in the size and shape of the Mg clips throughout the two-month implantation period were observed. It also can be seen that there is no significant corrosion occurred at the top corner part of the clamped magnesium alloy clips, indicating that clips degraded homogeneously, resulting this new designed Mg–3Zn-0.2Ca alloy clip can successfully withstand the blood pressure after occlusion. Fig. 8b and e shows enlarged surface morphologies of the clips after implantation for two months. Some corrosion degradation products are deposited in a honeycomb-like etched pit instead of being peeled off immediately, thereby inhibiting further corrosion of the clips, which in accord with the tendency of H_2 gas generation from the X-ray images results. EDS results (Fig. 8c) show corrosion products were abundant in O, Ca, P, Zn and Mg, which benefited the healing of blood vessels. Fig. 8f presents the weight loss of Mg–Zn–Ca clips as a function of implanted periods. During the initial 2 months of implantation, all

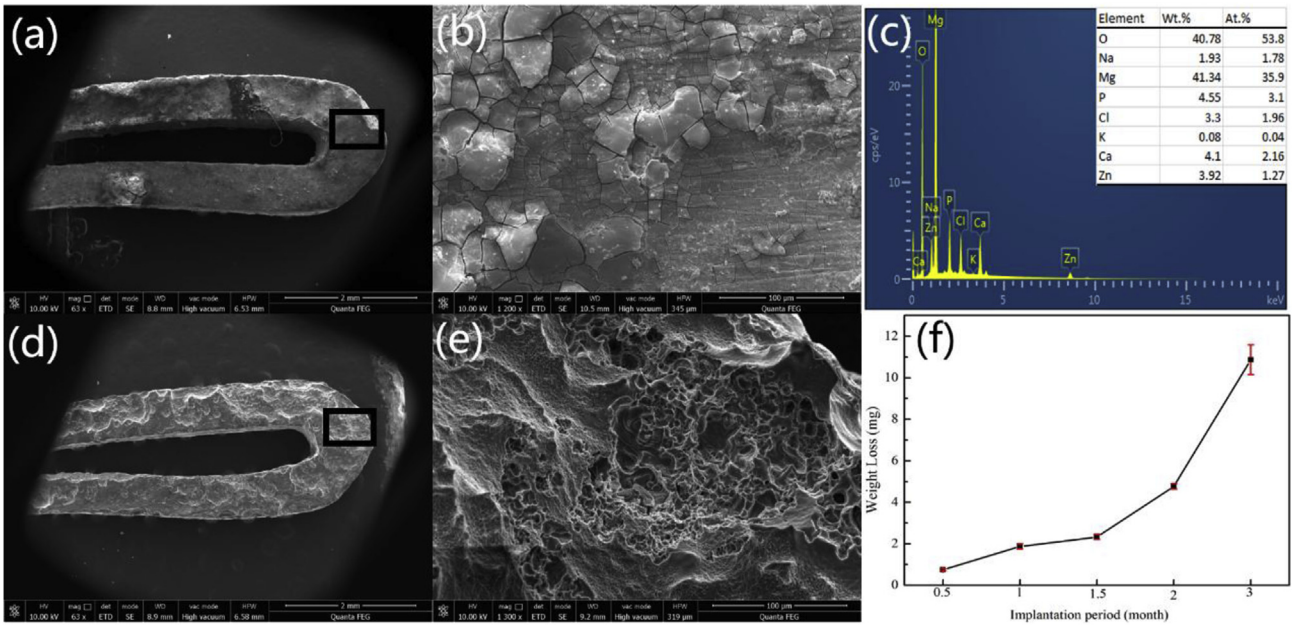

Fig. 8. SEM images of clip implanted for 2 months: immediately after removal (a) and after corrosion products were removed (d). The enlarged view of the clip (b, e) at 63 × . EDS spectrum analysis result of corrosion products in (c). Weight loss curve of clips at each implanted period (f).

clips showed similar degradation rates. There is a significant increase in the rate of degradation during the implantation period from 2 months to 3 months, which suggests the occurrence of pitting corrosion.

4. Conclusion

In this study, newly designed Mg–Zn–Ca alloy hemostatic clips were developed to overcome the drawbacks of the non-degradable Ti clips. These Mg–Zn–Ca clips can successfully ligated carotid artery and no blood leakage occurred after surgery. During the degradation of these clips, no tissue inflammation around the clips and a small amount of H_2 gas formation were observed. Due to the effect of arterial blood, the degradation rate of the clip implanted near the heart faster than that of clip implanted far away from the heart. Histological analysis and various blood biochemical parameters at different times after clip implantation also confirmed no tissue inflammation around the clips. Therefore, the newly designed Mg–3Zn-0.2Ca clips are expected as a good candidate for biodegradable hemostasis clip.

Conflict of interest

The authors declared that they have no conflicts of interest to this work. We declare that we do not have any commercial or associative interest that represents a conflict of interest in connection with the work submitted.

Acknowledgements

The authors acknowledge the financial support for this work from the National Natural Science Foundation of China (U1764254) and key projects supported by Tianjin Science and Technology (15ZCZDSY00920). We also thank Dr. Yizeng Wang from Tianjin Medical University General Hospital for support with animal implantation experiments. The authors are also grateful for the equipment provided by Tianjin Tianhe Hospital.

References

[1] G. Wang, J. Song, Comprehensive nursing intervention effect in treating hypertensive cerebral hemorrhage by minimally invasive surgery, Biomed. Res. 28 (2017) 8857–8860.
[2] W. Li, Y. Li, H. Lin, Curative effect of minimally invasive surgery on palmar and foot hyperhidrosis and its influence on serum-related cytokines and immunoglobulins, Exp. Ther. Med. 15 (2018) 3759–3764.
[3] W.J. Choi, J.H. Moon, J.S. Min, Y.K. Song, S.A. Lee, J.W. Ahn, S.H. Lee, H.C. Jung, Real-time detection system for tumor localization during minimally invasive surgery for gastric and colon cancer removal: in vivo feasibility study in a swine model, J. Surg. Oncol. 117 (2018) 699–706.
[4] S. Delibegović, M. Katica, F. Latić, J. Jakić-Razumović, A. Koluh, M.T.M. Njoum, The biocompatilbity of titanum clips after laparoscopic appendectomy, BH Surgery 3 (2013) 23–36.
[5] A. Ew, Absorbable metal clips as substitutes for ligatures and deep sutures in wound closure, Jama 4 (1917) 278–281.
[6] J. Szewczenko, J. Marciniak, W. Kajzer, A. Kajzer, Evaluation of corrosion resistance of titanium alloys used for medical implants, Arch. Metall. Mater. 61 (2016) 695–700.
[7] Z. Yu, G. Yang, W. Zhang, J. Hu, Investigating the effect of picosecond laser texturing on microstructure and biofunctionalization of titanium alloy, J. Mater. Process. Technol. 255 (2018) 129–136.
[8] N. Ikeo, R. Nakamura, K. Naka, T. Hashimoto, T. Yoshida, T. Urade, K. Fukushima, H. Yabuuchi, T. Fukumoto, Y. Ku, T. Mukai, Fabrication of a magnesium alloy with excellent ductility for biodegradable clips, Acta Biomater. 29 (2016) 468–476.
[9] T. Yoshida, T. Fukumuto, T. Urade, M. Kido, H. Toyama, S. Asari, T. Ajiki, N. Ikeo, T. Mukai, Y. Ku, Development of a new biodegradable operative clip made of a magnesium alloy: evaluation of its safety and tolerability for canine cholecystectomy, Surgery 161 (2017) 1553–1560.
[10] L. Filli, R. Luechinger, T. Frauenfelder, S. Beck, R. Guggenberger, N. Farshad-Amacker, G. Andreisek, Metal-induced artifacts in computed tomography and magnetic resonance imaging: comparison of a biodegradable magnesium alloy versus titanium and stainless steel controls, Skelet. Radiol. 44 (2015) 849–856.
[11] R.D. Klein, G. Jessup, F. Ahari, R.J. Connolly, S.D. Schwaitzberg, Comparison of titanium and absorbable polymeric surgical clips for use in laparo-scopic cholecystectomy, Surg. Endosc. 8 (1994) 753–758.
[12] K. Müller, E. Valentine-Thon, Hypersensitivity to titanium: clinical and laboratory evidence, Neuroendocrinol. Lett. 27 (1) (2006) 31–35 Suppl 1.
[13] Y.F. Zheng, X.N. Gu, F. Witte, Biodegradable metals, Mater. Sci. Eng. R. 77 (2014) 1–34.
[14] F. Witte, The history of biodegradable magnesium implants: a review, Acta Biomater. 23 (2015) S28–S40.
[15] L. Filli, R. Luechinger, T. Frauenfelder, et al., Metal-induced artifacts in computed tomography and magnetic resonance imaging: comparison of a biodegradable magnesium alloy versus titanium and stainless steel controls[J], Skelet. Radiol. 44 (6) (2015) 849–856.
[16] Z. Wu, R. Ahmad, B. Yim, S. Sandlöbes, W.A. Curtin, Mechanistic origin and prediction of enhanced ductility in magnesium alloys, Science 359 (2018) 447–452.
[17] Y. Min, L. Debao, Z. Runfang, C. Minfang, Microstructure and properties of Mg-3Zn-0.2Ca alloy for biomedical application, Rare Metal Mater. Eng. 47 (2018) 0093–0098.
[18] H. Li, D. Liu, Y. Zhao, F. Jin, M. Chen, The influence of Zn content on the corrosion and wear performance of Mg-Zn-Ca Alloy in simulated body fluid, J. Mater. Eng. Perform. 25 (2016) 3890–3895.
[19] N. Ikeo, R. Nakamura, K. Naka, et al., Fabrication of a magnesium alloy with

excellent ductility for biodegradable clips[J], Acta Biomater. 29 (2016) 468–476.
[20] H. Bai, X. He, P. Ding, D. Liu, M. Chen, Fabrication, microstructure, and properties of a biodegradable Mg-Zn-Ca clip[J], J. Biomed. Mater. Res. B Appl. Biomater. 107 (5) (2019) 1741–1749.
[21] ISO 10993-5:Biological Evaluation of Medical Devices-Part 5: Tests for in Vitro Cytotoxicity.
[22] Yuanming Gao, Lizhen Wang, Linhao Li, et al., Effect of stress on corrosion of high-purity magnesium in vitro and in vivo[J], Acta Biomater. 83 (2019) 477–486.
[23] X.N. Gu, S.S. Li, X.M. Li, Y.B. Fan, Magnesium based degradable biomaterials: a review, Front. Mater. Sci. 8 (3) (2014) 200–218.
[24] A. Atrens, G.L. Song, M. Liu, Z.M. Shi, F.Y. Cao, M.S. Dargusch, Review of recent developments in the field of magnesium corrosion, Adv. Eng. Mater. 17 (4) (2015) 400–453.